ACS APPLIED MATERIALS & INTERFACES

Article

Electrochemical detection of amyloid-# oligomers based on the signal amplification of a network of silver nanoparticles

Ning Xia, Xin Wang, Binbin Zhou, Yangyang Wu, Wenhui Mao, and Lin Liu

ACS Appl. Mater. Interfaces, **Just Accepted Manuscript** • DOI: 10.1021/acsami.6b05423 • Publication Date (Web): 14 Jul 2016

Just Accepted

ACS Publications

ACS Applied Materials & Interfaces is published by the American Chemical Society.
1155 Sixteenth Street N.W., Washington, DC 20036

Electrochemical detection of amyloid-β oligomers based on the signal amplification of a network of silver nanoparticles

Ning Xia, Xin Wang, Binbin Zhou, Yangyang Wu, Wenhui Mao, Lin Liu*

Henan Province of Key Laboratory of New Optoelectronic Functional Materials, College of Chemistry and Chemical Engineering, Anyang Normal University, Anyang, Henan 455000, People's Republic of China

*Corresponding author. *E-mail address*: liulin@aynu.edu.cn; *Tel:* +86 732 330 0925

Abstract: Amyloid-β oligomers (AβOs) are the most important toxic species in the brain of Alzheimer's disease (AD) patient. AβOs, therefore, are considered reliable molecular biomarkers for the diagnosis of AD. Herein, we reported a simple and sensitive electrochemical method for the selective detection of AβOs using silver nanoparticles (AgNPs) as the redox reporters and PrP(95–110), an AβOs-specific binding peptide, as the receptor. Specifically, adamantine (Ad)-labeled PrP(95–110), denoted as Ad-PrP(95–110), induced the aggregation and color change of AgNPs and the follow-up formation of a network of Ad-PrP(95–110)-AgNPs. Then, Ad-PrP(95–110)-AgNPs were anchored onto a β-cyclodextrin (β-CD)-covered electrode surface through the host-guest interaction between Ad and β-CD, thus producing an amplified electrochemical signal through the solid-state Ag/AgCl reaction by the AgNPs. In the presence of AβOs, Ad-PrP(95–110) interacted specifically with the AβOs, thus losing the capability to bind AgNPs and to induce the formation of an AgNPs-based network on the electrode surface. Consequently, the electrochemical signal decreased with an increase in the concentration of AβOs in the range of 20 pM to 100 nM. The biosensor had a detection limit of 8 pM and showed no response to amyloid-β monomers (AβMs) and fibrils (AβFs). Based on the well-defined and amplified electrochemical signal of the AgNPs-based network architecture, these results should be valuable for the design of novel electrochemical biosensors by marrying specific receptors.

Keywords: Electrochemical biosensors; silver nanoparticles; amyloid-β oligomers; peptide; colorimetric assay; host−guest interaction

INTRODUCTION

The most common cause of dementia is Alzheimer's disease (AD). One in 85 elderly people are expected to develop AD by 2050. The disease is characterized by loss of memory and cognitive decline and it has been associated with senile plaque in the brain.[1] Amyloid-β (Aβ) peptides, which have 39–43 amino acid residues, are the major constituent of senile plaque. Aβ monomers (AβMs) in their native forms result from proteolytic cleavage of amyloid precursor protein (APP) by β- and γ-secretase. AβMs can coalesce to form soluble, small oligomers (AβOs). These oligomers can reorganize and assemble into insoluble, long, often twisted thread-like fibrils (AβFs). There is good evidence that soluble AβOs are the most important toxic species that possesses the ability to disrupt membrane functions and thereby can induce neuronal damage in AD.[2,3] AβOs, therefore, are considered reliable molecular biomarkers for the diagnosis of AD.[4,5] They are also crucial therapeutic intervention targets. An enzyme-linked immunosorbent assay (ELISA) is the currently used method for the clinical detection of AβOs.[6-8] However, a typical sandwiched ELISA requires one to two days, the use of a relatively expensive enzyme-linked antibody and carcinogenic substrates for the chemiluminescent detection step.[9] For this consideration, a few techniques, including nanoparticles-based immunoassays,[10-12] electrochemistry,[10-14] surface-enhanced Raman spectroscopy (0.1 μM),[15] fluorescence[16] and localized surface plasmon resonance (LSPR)[17,18] have been recently utilized to detect AβOs. They are reliable but are labor intensive, require complicated instruments or less stable and relatively expensive antibodies and/or lack sensitivity. Therefore, for the early diagnosis of AD, it is highly desirable to develop simple, cost-effective and sensitive methods that are amenable to the selective detection of AβOs in body fluids.

It is not known whether specific receptors mediate the adverse effects of AD even though AβOs cause memory impairment by disrupting synaptic junctions between neurons, which has been associated with memory-related functions. Cellular prion protein (PrP^C, a membrane-bound glycoprotein) is present in the central nervous system. Recently, an expression cloning screen technique identified PrP^C as the receptor for binding synthetic AβOs with high affinity, indicating that PrP^C may be a functional receptor for AβOs.[19-21] A few works have also suggested that the core region of PrP^C for the AβOs/PrP^C interaction is PrP(95–110). These residues are located within the unstructured N-terminal region of PrP^C with an amino acid

sequence of THSQWNKPSKPKTNMK.[19,22-24] Using different analytical techniques, including surface plasmon resonance (SPR), dissociation-enhanced lanthanide fluorescence immunoassays (DELFIA) and cellular binding assays, several groups have suggested that the dissociation constant (K_d) for the AβOs/PrP^C interaction is in the subnanomolar range.[22,23,25] They also confirmed that the binding is highly specific for AβOs but not for AβMs and AβFs. The findings suggest that PrP(95–110) could be used as a receptor for the development of selective and antibody-free biosensors for AβOs detection.

Electrochemical biosensors have been used widely in recent years in clinical diagnosis, food quality control, biomedical research and environmental monitoring.[26-28] Their usefulness is due to their properties of high sensitivity, simplicity, compatibility with miniaturization and rapid responses. The increasing demand for the detection of ultralow amounts of analytes with electrochemical biosensors is pushing the enhancement of detection sensitivity through signal amplification. Usually, the amplified strategies include redox cycling, bioelectrocatalysis with enzymatic assays and metal nanoparticles.[29-32] Among of these protocols, metal nanoparticles have excellent potential for chemical and biological sensing. For example, silver nanoparticles (AgNPs) have been recently applied as the electrochemical biosensing elements used for signal readout through the solid-state Ag/AgCl reaction of AgNPs.[33-38] In particular, the AgNPs-based network architecture provides a well-defined and amplified electrochemical signal.[39-41] In this work, we found that PrP(95–110) can induce the aggregation and color change of AgNPs, whereas the introduction of AβOs prevented PrP(95–110)-triggered AgNPs aggregation. Inspired by our observations and the previous report that found that a AgNPs-based liquid-phase colorimetric assay could be converted into an enhanced surface tethered electrochemical analysis to significantly improve the detection sensitivity,[41] we believe that the above examples could be re-creations of an electrochemical platform for the sensitive and selective detection of AβOs. The use of the dual-functioning PrP(95–110) (binding to AβOs and inducing AgNPs aggregation) will obviate the utilization of expensive and less stable antibodies and the modification of analyte-binding receptors onto nanoparticles.

EXPERMENTAL SECTION

Chemicals and reagents. The Aβ peptide with 42 amino acid residues ($A\beta_{1-42}$), 6-mercapto-1-hexanol (MCH), tris(carboxy-ethyl)phosphine (TCEP), bovine serum albumin (BSA), immunoglobin G (IgG), thrombin, α-synuclein, sodium borohydride ($NaBH_4$), 1,1,1,3,3,3-hexafluoro-2-propanol (HFIP), KH_2PO_4 and K_2HPO_4 were purchased from Sigma-Aldrich. Trisodium citrate was obtained from Sangon Biotech. Co., Ltd. (Shanghai, China). Silver nitrate ($AgNO_3$) was purchased from Aladdin Reagent Company (Shanghai, China). Mercapto-β-cyclodextrin (β-CD-SH) was provided by Shandong Zhiyuan Biotechnology, Ltd. (China). PrP(95–110), with the sequence THSQWNKPSKPKTNMK and adamantine-labeled PrP(95–110), denoted as Ad-PrP(95–110), were synthesized and purified by ChinaPeptides Co., Ltd. (Shanghai, China). The Ad-PrP(95–110) stock solution (1 mM) was prepared with deionized water and diluted with a 2 mM acetate buffer or phosphate-buffered saline solution (PBS buffer) before use. The buffer solutions at pH 3.8 and 4.5 were prepared by acetic acid and sodium acetate, and those at pH 6.4, 7.2 and 8.1 were prepared by KH_2PO_4 and K_2HPO_4. The deionized water was purified by a Millipore system.

Synthesis of AgNPs. AgNPs were synthesized by the chemical reduction of Ag^+ ions using $NaBH_4$ as the reducing reagent and trisodium citrate as the stabilizer. Briefly, 1 mL of a 10 mM $AgNO_3$ solution and 1 mL of a 10 mM trisodium citrate solution were added to 36.8 mL of deionized water under vigorous stirring. This step was followed by the addition of 1.2 mL of freshly prepared 10 mM $NaBH_4$. The color of the solution gradually changed to yellow, indicating the formation of the AgNPs. After the reaction proceeded for approximately 10 min, the resulting colloid was aged for 2 days at 4 °C. The morphology of the AgNPs was observed by a FEI Tecnai G2 T20 transmission electron microscope (TEM). The average size of AgNPs was determined to be 11.7 ± 1.6 on a Nano ZS laser scattering particles size analyzer (Malvern Instruments Ltd, Malvern, Worcestershire, UK) (Figure S1). The concentration of the AgNPs was calculated to be 8.5 nM according to the AgNPs size and the Ag^+ concentration.

Preparation of soluble AβOs. Soluble AβOs were prepared as in previous reports.[11,21] In brief, HFIP was used to dissolve the $A\beta_{1-42}$ lyophilized powder at a concentration of 1 mg/mL. The solution was then sonicated for 10 min to monomerize the pre-existing aggregates. The resulting $A\beta_{1-42}$ was reconstituted in 20 mM NaOH to

a concentration of 2 mM. After dilution with a phosphate-buffered saline solution (PBS buffer, 10 mM, pH.2), the final concentration was 50 μM. The sample was diluted with 2 mM PBS buffer at pH 7.2 to the desired concentration for the experiments after incubation at 25 °C. The peptide concentration was determined from the UV-vis spectrum using the extinction coefficient of 1410 M^{-1} cm^{-1} at 276 nm. The concentrations of the AβOs in this study were calculated as the equivalent concentrations to monomers.

The Aβ species in different forms were characterized by Atomic Force Microscopy (AFM) with a Dimension Edge microscope (Bruker Nano Inc., Santa Barbara, CA) equipped with a tapping mode. Aliquots of $Aβ_{1–42}$ at a concentration of 50 μM were removed at set times during incubation. They were then put on newly peeled mica and remained in contact with the mica substrate for 15 min. Water was used to wash the slides to remove residual salt and then the slides were dried under a very gentle nitrogen stream previous to imaging.

Ad-PrP(95–110)-triggered AgNPs aggregation. 250 μL of the diluted AgNPs dispersion at a concentration of 4.8 nM was added to 250 μL of Ad-PrP(95–110) solution at a given concentration. After incubation for 5 min, color changes were observed with the naked eye, and the UV-vis absorption spectra were recorded with a Cary 50 spectrophotometer using a 1 cm quartz spectrophotometer cell. The photographs were taken with a Sony Cyber-Shot digital camera. To investigate the effect of the Aβ sample (or the interfering proteins) on Ad-PrP(95–110)-triggered AgNPs aggregation, 200 μL of the Ad-PrP(95–110) solution was first mixed with 50 μL of the Aβ solution (or the interfering proteins) in a test tube. Then, the mixture was incubated with 250 μL of the diluted AgNPs at room temperature for 5 min. The color change and the absorption spectra of the mixture solution were also recorded by the digital camera and the UV-vis spectrophotometer, respectively.

Preparation of sensing electrodes. The cyclodextrin-covered electrodes were obtained by incubating the cleaned plate gold electrodes with a mixed solution of 20 μM β-CD-SH and 50 μM TCEP overnight. After having been rinsed with water, the electrodes were soaked in a 1 mM MCH solution for 10 min. The unreacted gold surface would be blocked by MCH. The resulting MCH/β-CD-modified electrodes were stored in a clean environment at 4 °C for use.

Effect of the concentrations of Ad-PrP(95–110) and AgNPs. To investigate the

effect of the concentration ratio of Ad-PrP(95–110) to AgNPs on the electrochemical signal, 50 μL of Ad-PrP(95–110) solutions at different concentrations were incubated with 50 μL of AgNPs at room temperature for 5 min. Then, 10 μL of the mixed solutions were cast onto the electrode surface for 30 min. After the electrode was rinsed with water, linear-sweep voltammetry (LSV) was performed in a 1 M KCl solution on a CHI 660E electrochemical workstation (CH Instruments, Shanghai, China). The auxiliary electrode is a platinum wire. The reference electrode is an Ag/AgCl. To investigate the effect of the concentration of the network architecture of Ad-PrP(95–110)-AgNPs on the electrochemical signal, Ad-PrP(95–110)-AgNPs at an optimal concentration ratio of Ad-PrP(95–110) to AgNPs were diluted to different concentrations. Then, 10 μL of the diluted nanocomposites were cast onto the electrode surface for 30-minutes incubation. After being rinsed with water, the electrode was placed in 1 M KCl for the LSV measurement.

Electrochemical detection of AβOs. For the detection of AβOs, 10 μL of the Aβ sample at a given concentration was first mixed with 40 μL of Ad-PrP(95–110) solution at room temperature. After the reaction proceeded for 5 min, 50 μL of the AgNPs solution was added to the Ad-PrP(95–110)/Aβ mixed solution and incubated for additional 5 min. After the electrode was incubated with the AβOs/ Ad-PrP(95–110)/AgNPs mixture for 30 min and rinsed with water, the electrochemical signal was collected using LSV in a 1 M KCl solution.

For the specificity studies, α-synuclein at the concentration of 50 μM was incubated in PBS (pH 7.2, 10 mM) for 24 h before mixing with Ad-PrP(95–110). The other proteins were prepared freshly and used without additional treatment. The serum sample from one yellow staff (male, 53 years old) was obtained from the health center of Anyang Normal University (Anyang, China) and diluted by the desired fold with the PBS buffer.

SPR detection. The fabrication and modification of SPR sensing chips were carried out as follows. The cyclodextrin-covered chips were prepared by immersing the gold films in 50 μM of a β-CD-SH solution containing 50 μM TCEP overnight. After being washed thoroughly with water, the films were soaked in 1 mM of a MCH solution for 10 min to block the unreacted gold surface. These modified chips were then washed with water and soaked in an Ad-PrP (95–110) solution for 30 min. The PrP(95–110) sensor chip was made by linking Ad-PrP(95–110) molecules onto the

MCH/β-CD-modified chip surface through the interaction of Ad and β-CD. The chip was assembled into the SPR prism with an index-matching fluid after surface modifications. Once a stable baseline was obtained, the Aβ sample was delivered onto the SPR flow cell using a syringe pump. The signals were measured using a BI-SPR 3000 system (Biosensing Instrument Inc., Tempe, AZ).

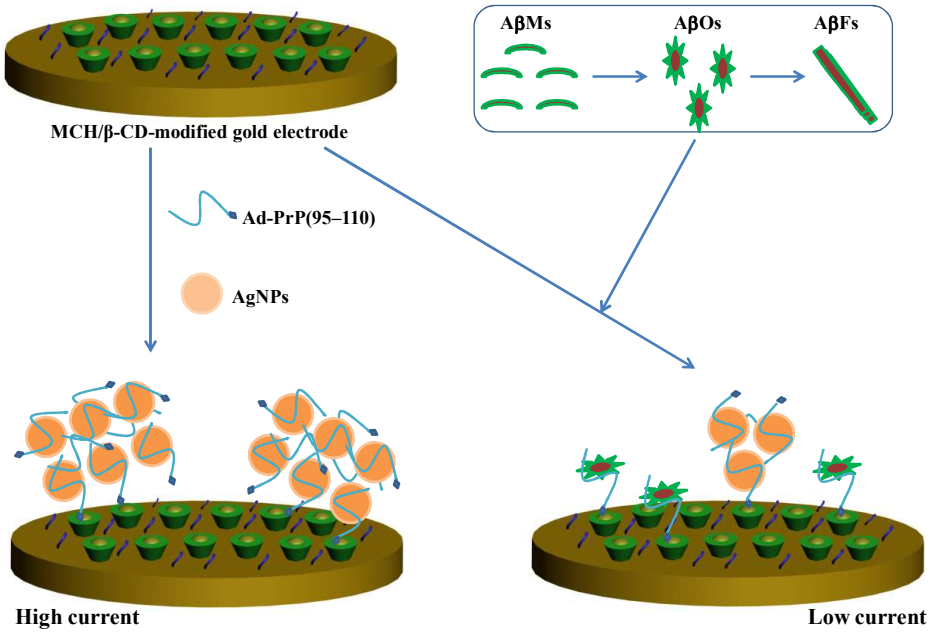

Figure 1. Schematic illustration of the electrochemical method for the selective detection of AβOs using AgNPs as the redox reporters and Ad-PrP(95–110) as the receptor.

RESUTLS AND DISCUSSION

The host−guest interaction has been extensively applied in this bioanalysis.[42,43] To achieve signal amplification and improve the analytical performance of the competitive assay, a small molecule, adamantine (Ad), was used as the guest to label PrP(95-110), and the detection platform was designed via supramolecular chemistry. As shown in Figure 1, the AβOs-specific binding peptide with a sequence of Ad-THSQWNKPSKPKTNMK Ad-PrP(95–110) can be anchored onto the MCH/β-CD-modified electrode surface through the interaction of Ad and β-CD,[44,45] and it can be adsorbed onto the surface of AgNPs to induce the aggregation and color change of AgNPs suspensions. The resulting network architecture of Ad-PrP(95–110)-AgNPs formed on the electrode surface will produce an amplified

electrochemical signal through the solid-state Ag/AgCl reaction from AgNPs. Upon the addition of an Aβ sample to the Ad-PrP(95–110) solution, Ad-PrP(95–110) would interact specifically with AβOs, thus losing the capability to bind AgNPs and to induce the formation of an AgNPs-based network architecture. Moreover, the resulting Ad-PrP(95–110)-AβOs can also attach onto the MCH/β-CD-modified electrode surface through the interaction between Ad and β-CD, which will thus prevent the capture of Ad-PrP(95–110)-AgNPs. Consequently, the electrochemical signal from the oxidation of the AgNPs will decrease with an increase in the AβOs concentration.

To demonstrate the feasibility of this method, Ad-PrP(95–110)-triggered color and absorbance changes in the AgNPs suspension in the absence and presence of different aggregation states of Aβ were first investigated by the naked eye and with an UV-Vis spectrophotometer. As shown in Figure 2A, the light-yellow AgNPs solution (tube 1) exhibited an absorption peak at 406 nm (black curve). Upon the addition of Ad-PrP(95–110), the color of the AgNPs suspension changed from light yellow to red (tube 2). Meanwhile, the original absorbance of the AgNPs suspension at 406 nm decreased. At the same time, a new absorbance peak at approximately 520 nm obviously increased (red curve), indicating that the aggregation of the AgNPs was induced by Ad-PrP(95–110). The result is understandable since Ad-PrP(95–110) contains four positively charged lysine residues and no negatively charged amino-acid residue is included in the sequence. So it was readily adsorbed onto the surface of negatively charged AgNPs through the electrostatic interaction. The effect of reaction temperature and solution pH on the Ad-PrP(95–110)-triggered AgNPs aggregation was also investigated. The A_{520}/A_{406} ratio (A_{520} and A_{406} represent the absorption intensity of AgNPs at 520 nm and 406 nm, respectively) was used to evaluate the effect. We found that solution temperature in the range of 15 ~ 45 °C shows no significant influence on the stability of AgNPs and the A_{520}/A_{406} ratio (Figure S2), AgNPs exhibits low absorption ability at pH below 5.7, and A_{520}/A_{406} reaches the maximum in the pH range of 6.4 ~ 7.2 (Figure S3). Thus, the following detection assays were carried out in a physiological pH 7.2 buffer solution at room temperature.

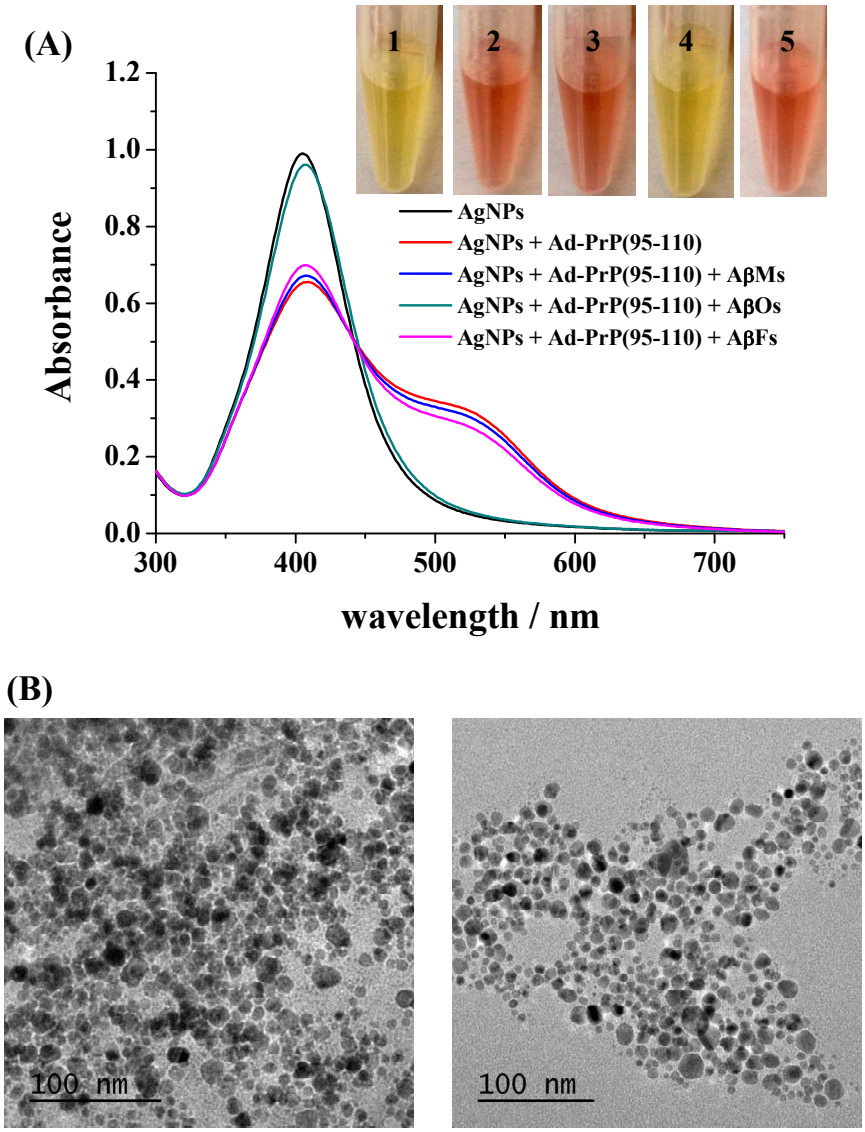

Figure 2. (A) The UV–vis absorption spectra of AgNPs at pH 7.2 in various systems. The final concentrations of AgNPs, Ad-PrP(95–110) and Aβ samples were 2.4 nM, 0.1 μM and 2.5 μM, respectively. The inset shows the photographic images of the AgNPs in the dispersed and aggregated states. (B) TEM images of the AgNPs in the presence of Ad-PrP(95–110) (left) and Ad-PrP(95–110)/AβOs (right).

For the assays of AβMs (blue curve, tube 3), AβOs (olive curve, tube 4) and AβFs (magenta curve, tube 5), only in the presence of AβOs did the color of the AgNPs remain light yellow, and one absorption peak at 406 nm was observed. The inhibition of Ad-PrP(95–110)-triggered AgNPs aggregation can be attributed to the specific interaction between PrP(95–110) and AβOs. This result was further confirmed by

TEM observations; there was significant aggregation of AgNPs in the presence of Ad-PrP(95–110) alone and monodisperse AgNPs in the presence of Ad-PrP(95–110) and AβOs (Figure 2B). Moreover, we found that the presence of proteins (e.g. BSA, IgG, thrombin and α-synuclein) did not inhibit the Ad-PrP(95–110)-triggered AgNPs aggregation (Figure S4), indicating the high specificity of the colorimetric assay to AβOs. We also investigated the effect of the concentrations of Ad-PrP(95–110) and AβOs on the absorption change of AgNPs. With increased concentrations of Ad-PrP(95–110), the A_{520}/A_{406} ratio increased in the concentration range of 1 ~ 200 nM (Figure S5). Conversely, A_{520}/A_{406} decreased with increased concentrations of AβOs in a linear concentration range of 0.01 ~ 2.5 μM (Figure S6).

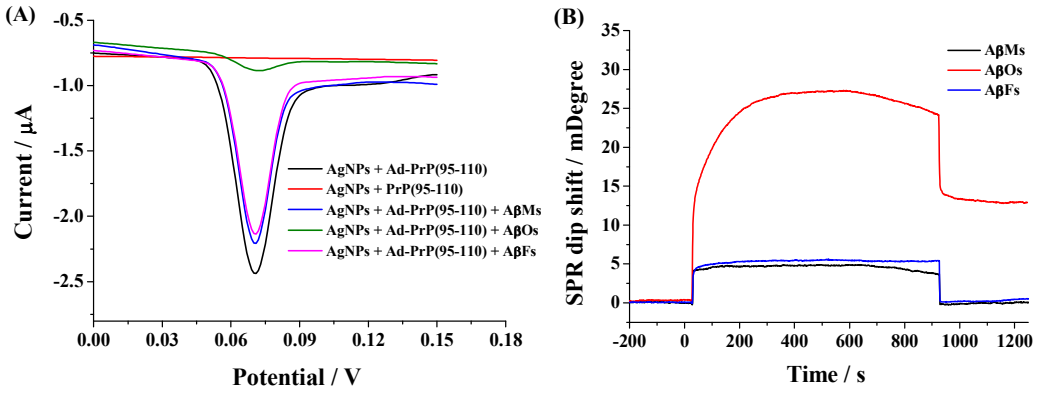

Figure 3. (A) LSV responses acquired by the MCH/β-CD-modified electrodes after incubation in different solutions. The scan rate was 0.1 V/s. The final concentrations of the AgNPs, Ad-PrP(95–110), PrP(95–110) and Aβ were 2.4 nM, 0.1 μM, 0.1 μM and 2.5 μM, respectively. (B) The binding of different forms of Aβ to PrP(95–110) immobilized on the SPR chip. The concentration of the Aβ sample used was 5 μM.

Figure 3A shows the LSV responses acquired by the MCH/β-CD-modified electrodes after incubation with mixed solutions of Ad-PrP(95–110) and AgNPs in the absence and presence of different forms of Aβ species. After Ad-PrP(95–110)-AgNPs (black curve) were captured, the electrochemical response revealed a reduction peak at approximately 70 mV. We also noticed that although PrP(95–110) can induce the aggregation of the AgNPs, the MCH/β-CD-modified electrode exhibits no electrochemical signal after incubation with PrP(95–110)-AgNPs (red curve). Thus, the reduction peak should be attributed to the solid-state Ag/AgCl reaction from

Ad-PrP(95–110)-AgNPs, and the capturing of the network architecture of AgNPs was strictly dependent upon the interaction of Ad and β-CD. The blue, olive and magenta curves are the representative LSV responses collected by the MCH/β-CD-modified electrodes after incubation with mixed solutions of Aβ sample, Ad-PrP(95–110) and AgNPs. It was observed that AβOs resulted in a much attenuated peak current (cf. black and olive curves), while no significant changes were observed for AβMs (blue curve) and AβFs (magenta curve). The slight decrease in the current of these two curves is probably due to the existence of small amounts of AβOs in the solution during sample preparation. To further confirm that the proposed biosensor maintains a conformation-specific recognition mechanism and was highly selective for AβOs, we also conducted a SPR experimental to investigate the interaction between AβOs and PrP(95–110). As shown in Figure 3B, in contrast to AβOs, no binding was detected for AβMs or AβOs. This result agrees with that obtained by the CM5 SPR sensor chip, indicating that the sensor is selective for AβOs but not for AβMs or AβFs. These results are acceptable because the secondary structure of Aβ is indispensable for the recognition of PrP(95–110).

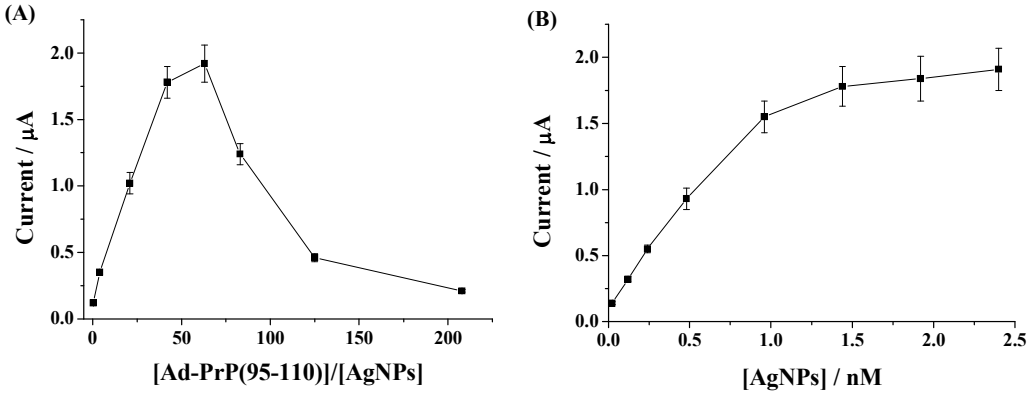

Figure 4. The effect of the concentration ratio of Ad-PrP(95–110) to AgNPs (A) and the final concentration of AgNPs (B) on the LSV peak current. The absolute errors were deduced from three replicate measurements and are shown as the error bars.

To demonstrate the generality of our design using AgNPs as the redox reporters and Ad-PrP(95–110) as the receptor for AβOs detection, several experimental conditions were optimized. Note that higher concentration of Ad-PrP(95–110) could induce

greater aggregation of the AgNPs (Figure S5). However, a higher concentration of Ad-PrP(95–110) would require a higher concentration of AβOs in the competitive assay. More importantly, free Ad-PrP(95–110) in solution will compete with the network architecture of Ad-PrP(95-110)-AgNPs to bind β-CD on the electrode surface. This will reduce the electrochemical signal and deteriorate the detection sensitivity. Thus, the concentration ratio of Ad-PrP(95–110) to AgNPs ([Ad-PrP(95–110)]/[AgNPs]) was first examined. As shown in Figure 4A, the influence of the concentration ratio of Ad-PrP(95–110) to AgNPs on the signal had an inverted-V shape, which was initially increased by increasing the concentration ratio of Ad-PrP(95–110) to AgNPs until the maximum value appeared at 63:1, followed by a sharp decrease. This decrease is indicative of the competitive binding of Ad-PrP(95–110)-AgNPs and a low amount of free Ad-PrP(95–110) in the solution to β-CD on the electrode surface. Thus, 63:1 was selected as the optimal concentration ratio of Ad-PrP(95–110) to AgNPs in the following detection assays. Then, the electrochemical signals were collected after the sensing electrodes were coated with various concentrations of Ad-PrP(95–110)/AgNPs. It was found that the current gradually increased upon increasing concentrations of Ad-PrP(95–110)/AgNPs and began to level off beyond 1.44 nM (AgNPs concentration) (Figure 4B). In the context of the optimal linear range of the current-concentration, AgNPs at a final concentration of 0.96 nM were used in the following competitive assays.

The incubation time for the formation of the AβOs also has a significant influence on the assay detection. The morphology of the Aβ species at different incubation times was first characterized using AFM, as shown in Figure 5A. We found that the current reached the minimum after a 24 h incubation, indicating that the optimal incubation time for the AβOs formation was approximately 24 h (Figure 5B). Thus, in the following detection assays, 24 h was set as the standard condition for AβOs preparation.

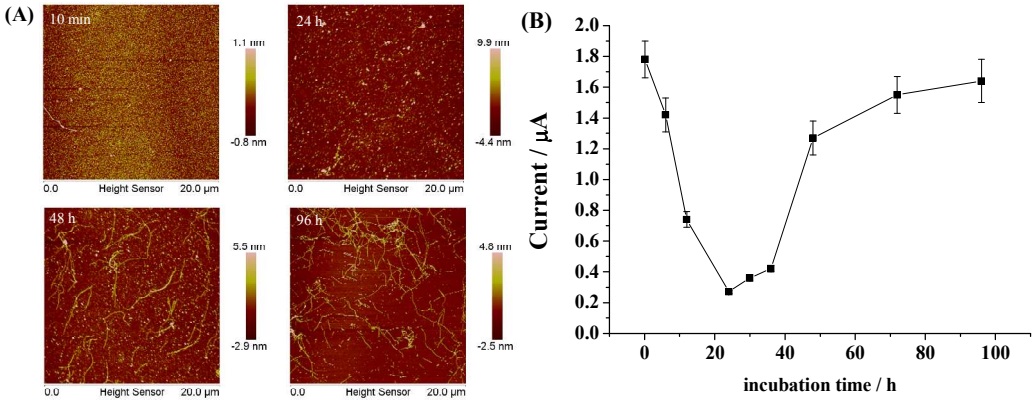

Figure 5. (A) The AFM images of the mica substrates after the attachment of the Aβ sample at different incubation times. (B) The dependence of the LSV current on different incubation times for AβOs formation. The final concentration of the Aβ sample (equivalent monomers) was 1 μM. The other experimental conditions were the same as those in Figure 3A.

Under the optimized experimental conditions, the AβOs quantitative assay was conducted by monitoring the LSV responses of the AgNPs-based network architecture formed on the electrode surface. As shown in Figure 6A, the current decreased with increasing AβOs concentration (equivalent monomers). The dependence of the LSV peak currents on the concentrations of Aβ is presented in Figure 6B. The current was inversely proportional to the Aβ concentration in the range from 20 pM to 100 nM. The regression equation was current (μA) = 1.42 – 0.012 [Aβ] (nM) (R = 0.997). The detection limit of the method was calculated to be 8 pM based on the slope of the dose-response curve and the standard deviation of the blank response (n = 11). The value was approximately 4 orders of magnitude lower than that of the aforementioned AgNPs-based colorimetric method (approximately 5 nM, Figure S6), demonstrating that the AgNPs-based liquid-phase colorimetric assay has been converted into an enhanced surface-tethered electrochemical assay. The detection limit of the AgNPs-based electrochemical method is comparable to (or lower than) that achieved by other methods, such as a molecular beacon (MB)-based fluorescent assay (3.57 nM),[16] square wave voltammetry (48 pM),[10] cyclic voltammetry by signal amplification of electrochemical–chemical–chemical redox cycling (3 pM),[11]

electrochemical impedance spectroscopy (100 pM),[12] a magnetic bead-droplet immunoassay (10 mg mL^{-1}),[46] surface-enhanced Raman spectroscopy (0.1 μM), [15] AgNPs-based localized surface plasmon resonance (LSPR) (0.1 pM) [17] and gold nanoparticles-based LSPR (1.5 pM).[18] Moreover, our method exhibited excellent selectivity for AβOs, does not need to modify nanoparticles, requires very simple sample handling and obviates the utilization of expensive and less stable antibodies, which improves the detection specificity and reduces the operation complexity, analysis time and detection cost. Additionally, the reproducibility of this electrochemical sensor was evaluated by analyzing the same AβOs sample on three parallel prepared electrodes and by analyzing three freshly prepared AβOs samples at the concentration of 50 nM. The relative standard deviations (RSDs, shown as the error bars in Figure 6B) for assays of the same AβOs sample on three different electrodes are all less than 11.4 %. The RSD of the values obtained by analyzing the three parallel prepared AβOs samples was found to be 14.7 %. The results suggested acceptable reproducibility of the proposed biosensor.

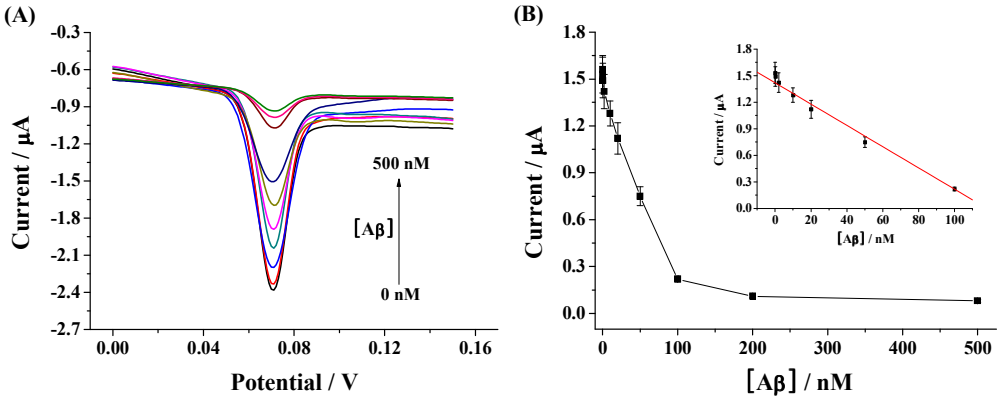

Figure 6. (A) The LSV responses acquired by the MCH/β-CD-modified electrodes after incubation with mixtures of Ad-PrP(95–110), AgNPs and different concentrations of AβOs (equivalent monomers: 0, 0.02, 0.2, 2, 10, 20, 50, 100, 200 and 500 nM). The final concentrations of Ad-PrP(95–110) and AgNPs were 60 nM and 0.96 nM, respectively. (B) The dependence of the LSV current on the Aβ concentration.

To explore the specificity of the proposed method, AβMs, AβFs and four interfering proteins (BSA, IgG, thrombin and α-synuclein) were chosen for the selectivity and

interference studies. As shown in Figure 7, compared to the control (bar 1), all the interferences caused a negative decrease in the current (bars 2 - 7). The high selectivity could be principally attributed to the specific binding capacity of PrP(95–110) to AβOs, not AβMs and AβFs. For the interfering proteins, this result is acceptable because they show no effect on the stability of AgNPs (even at micromolar concentration level),[47,48] and did not prevent the Ad-PrP(95–110)-triggered AgNPs aggregation (Figure S4). The results confirmed that the established electrochemical assay showed extraordinary selectivity towards AβOs detection. To further investigate the interference, AβMs, AβFs and these four interfering proteins were collectively mixed with AβOs for 2 min before incubation with PrP(95–110). We found that addition of the interferences to the AβOs solution had no meaningful influence on the current (bar 9) in comparison with that in the presence of AβOs only (bar 8). These results are indicative of the potential applicability of the sensing protocol for AβOs detection in biological matrix samples. To demonstrate the amenability of this electrochemical biosensor for quantifying AβOs in a serum sample, we first studied the effect of serum on the LSV current. It was found that the current decreased with the decrement of the dilution fold of the serum sample (Figure S7). The current matched the results in the buffer solution better when the serum sample was diluted by more than 50-fold. It is not clear why there was interference and this needs further analysis. However, the presence of some matrix components in serum solutions may be a possibility. The interference would be minimized by either the filtration steps or dilution of the samples. Diluting the samples should be a simple, practical application in our study. Our results showed, after comparing the results for the 2 % serum (bar 10) and buffer system (bar 8), that the assay also works in the diluted serum sample. Moreover, although organic dye-based fluorescence assays (e.g., thioflavin T or ThT) have been reported to monitor the formation of Aβ aggregates in laboratory studies, most of the dyes are incapable of discriminating AβOs from other Aβ aggregates.[49] Our methods may therefore allow quantification of AβOs in other types of laboratory studies (e.g., assessing the mechanism of Aβ aggregation/fibrillation processes and dynamics under

different experimental conditions and screening of novel inhibitors that could stop the formation of neurotoxic AβOs).

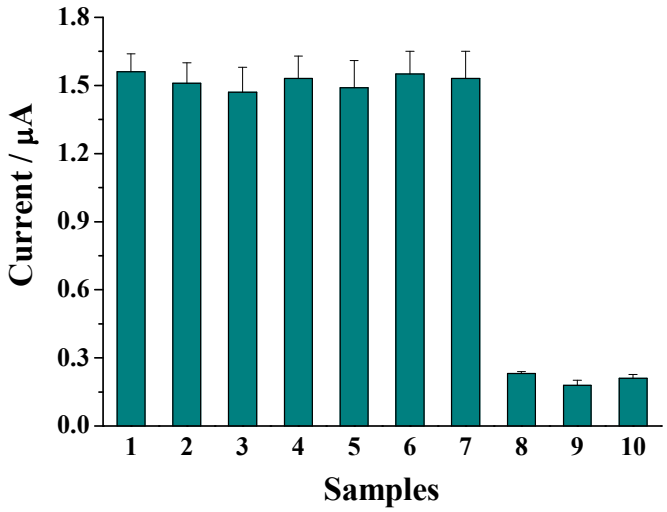

Figure 7. The selectivity and interference of the sensing protocol (bar 1, control; bar 2, AβMs; bar 3, AβFs; bar 4, BSA; bar 5, IgG; bar 6, thrombin; bar 7, α-synuclein; bar 8, AβOs in PBS; bar 9, AβOs with AβMs, AβFs and interfering proteins; bar 10, AβOs in 2 % serum). The final concentration of Aβ sample, BSA, IgG and thrombin was 100 nM, and that of α-synuclein was 5 μM. The other experimental conditions were the same as those in Figure 6.

CONCLUSION

This work presented a simple and sensitive electrochemical approach for the selective detection of AβOs by employing AgNPs as the redox reporters and an AβOs-specific peptide as the receptor. Compared with other methods for AβOs detection (e.g., immunoassay, LSPR and electrochemistry), our method exhibited excellent selectivity for AβOs because of the specific recognition of PrP(95–110) to AβOs and obviates the modification of nanoparticles for signal amplification and the utilization of expensive and less stable antibodies for molecular recognition. Moreover, because soluble AβOs are the most important toxic species in the brain of AD patient and the direct assay of AβOs would be more reliable for the early diagnosis of AD than assay of AβMs or AβFs, the proposed biosensor could potentially serve as a viable alternative for facile clinical diagnosis of AD. The result also confirmed that the AgNPs-based liquid-phase

colorimetric assay can be converted into an enhanced surface-tethered electrochemical assay. Taking advantage of the well-defined and amplified electrochemical signal of the AgNPs-based network architecture, our works should be helpful for the fabrication of novel electrochemical biosensors by marrying specific receptors.

AUTHOR INFORMATION

Corresponding Author

*Email: liulin@aynu.edu.cn. (L. Liu)

Author Contributions

The manuscript was written through contributions of all authors. All authors have given approval to the final version of the manuscript.

Notes

The authors declare no competing financial interest.

ACKNOWLEDGMENTS

Partial support of this work by the National Natural Science Foundation of China (Nos. 21205003, 21305004), the Joint Fund for Fostering Talents of National Natural Science Foundation of China and Henan Province (U1304205) and the Program for Science and Technology Innovation Talents at the University of Henan Province (15HASTIT001) is gratefully acknowledged.

REFERENCES

(1) Rauk, A., The Chemistry of Alzheimer's Disease. *Chem. Soc. Rev.* **2009**, *38*, 2698-2715.

(2) Glabe, C.G., Structural Classification of Toxic Amyloid Oligomers. *J. Biol. Chem.* **2008**, *283*, 29639-29643.

(3) Walsh, D.M.; Klyubin, I.; Fadeeva, J.V.; Cullen, W.K.; Anwyl, R.; Wolfe, M.S.; Rowan, M.J.; Selkoe, D.J., Naturally Secreted Oligomers of Amyloid Beta Protein Potently Inhibit Hippocampal Long-Term Potentiation in Vivo. *Nature* **2002**, *416*, 535-539.

(4) Cleary, J.P.; Walsh, D.M.; Hofmeister, J.J.; Shankar, G.M.; Kuskowski, M.A.;

Selkoe, D.J.; Ashe, K.H., Natural Oligomers of the Amyloid-β Protein Specifically Disrupt Cognitive Function. *Nature Neurosci.* **2005**, *8*, 79−84.

(5) Larson, M.E.; Lesné, S.E., Soluble Aβ Oligomer Production and Toxicity. *J. Neurochem.* **2012**, *120*, 125-139.

(6) Bruggink, K.A.; Jongbloed, W.; Biemans, E.A.L.M.; Veerhuis, R.; Claassen, J.A.H.R.; Kuiperij, H.B.; Verbeek, M.M., Amyloid-b Oligomer Detection by ELISA in Cerebrospinal Fluid and Brain Tissue. *Anal. Biochem.* **2013**, *433*, 112-120.

(7) Stenh, C.; Englund, H.; Lord, A.; Johansson, A.-S.; Almeida, C.G.; Gellerfors, P.; Greengard, P.; Gouras, G.K.; Lannfelt, L.; Nilsson, L.N.G., Amyloid-b Oligomers Are Inefficiently Measured by Enzyme-Linked Immunosorbent Assay. *Ann. Neurol.* **2005**, *58*, 147-150.

(8) Yang, T.; Hong, S.; O'Malley, T.; Sperling, R.A.; Walsh, D.M.; Selkoe, D.J., New Elisas with High Specificity for Soluble Oligomers of Amyloid β-Protein Detect Natural Aβ Oligomers in Human Brain but Not Csf. *Alzheimer's Dementia* **2013**, *9*, 99-112.

(9) Yu, Y.Y.; Zhang, L.; Li, C.L.; Sun, X.Y.; Tang, D.Q.; Shi, G.Y., A Method for Evaluating the Level of Soluble Beta-Amyloid$_{(1\text{-}40/1\text{-}42)}$ in Alzheimer's Disease Based on the Binding of Gelsolin to Beta-Amyloid Peptides. *Angew. Chem. Int. Ed.* **2014**, *53*, 12832-12835.

(10) Li, H.; Xie, H.; Cao, Y.; Ding, X.; Yin, Y.; Li, G., A General Way to Assay Protein by Coupling Peptide with Signal Reporter via Supermolecule Formation. *Anal. Chem.* **2013**, *85*, 1047-1052.

(11) Liu, L.; Xia, N.; Jiang, M.; Huang, N.; Guo, S.; Li, S.; Zhang, S., Electrochemical Detection of Amyloid-β Oligomer with the Signal Amplification of Alkaline Phosphatase plus Electrochemical-Chemical-Chemical Redox Cycling. *J. Electroanal. Chem.* **2015**, *754*, 40-45.

(12) Rushworth, J.V.; Ahmed, A.; Griffiths, H.H.; Pollock, N.M.; Hooper, N.M.; Millner, P.A., A Label-Free Electrical Impedimetric Biosensor for the Specific Detection of Alzheimer's Amyloid-Beta Oligomers. *Biosens. Bioelectron.* **2014**, *56*, 83-90.

(13) Li, H.; Cao, Y.; Wu, X.; Ye, Z.; Li, G., Peptide-Based Electrochemical Biosensor for Amyloid β 1–42 Soluble Oligomer Assay. *Talanta* **2012**, *93*, 358-363.

(14) Veloso, A.J.; Chow, A.M.; Ganesh, H.V.S.; Li, N.; Dhar, D.; Wu, D.C.H.;

Mikhaylichenko, S.; Brown, I.R.; Kerman, K., Electrochemical Immunosensors for Effective Evaluation of Amyloid-Beta Modulators on Oligomeric and Fibrillar Aggregation Processes. *Anal. Chem.* **2014**, *86*, 4901−4909.

(15) Guerrini, L.; Arenal, R.; Mannini, B.; Chiti, F.; Pini, R.; Matteini, P.; Alvarez-Puebla, R.A., SERS Detection of Amyloid Oligomers on Metallorganic-Decorated Plasmonic Beads. *ACS Appl. Mater. Interfaces* **2015**, *7*, 9420-9428.

(16) Zhu, L.; Zhang, J.; Wang, F.; Wang, Y.; Lu, L.; Feng, C.; Xu, Z.; Zhang, W., Selective Amyloid β Oligomer Assay Based on Abasic Site-Containing Molecular Beacon and Enzyme-Free Amplification. *Biosens. Bioelectron.* **2016**, *78*, 206-212.

(17) Haes, A.J.; Chang, L.; Klein, W.L.; Van Duyne, R.P., Detection of A Biomarker for Alzheimer's Disease from Synthetic and Clinical Samples Using A Nanoscale Optical Biosensor. *J. Am. Chem. Soc.* **2005**, *127*, 2264-2271.

(18) Kang, M.K.; Lee, J.; Nguyen, A.H.; Sim, S.J., Label-Free Detection of ApoE4-Mediated β-Amyloid Aggregation on Single Nanoparticle Uncovering Alzheimer's Disease. *Biosens. Bioelectron.* **2015**, *72*, 197-204.

(19) Balducci, C.; Beeg, M.; Stravalaci, M.; Bastone, A.; Sclip, A.; Biasini, E.; Tapella, L.; Colombo, L.; Manzoni, C.; Borsello, T.; Chiesa, R.; Gobbi, M.; Salmona, M.; Forloni, G., Synthetic Amyloid-β Oligomers Impair Long-Term Memory Independently of Cellular Prion Protein. *Proc. Nat. Acad. Sci. USA* **2010**, *107*, 2295-2300.

(20) Freir, D.B.; Nicoll, A.J.; Klyubin, I.; Panico, S.; Donald, J.M.M.; Risse, E.; Asante, E.A.; Farrow, M.A.; Sessions, R.B.; Saibil, H.R.; Clarke, A.R.; Rowan, M.J.; Walsh, D.M.; Collinge, J., Interaction Between Prion Protein and Toxic Amyloid β Assemblies Can Be Therapeutically Targeted at Multiple Sites. *Nat. Commun.* **2011**, *2*, 1-9.

(21) Laurén, J.; Gimbel, D.A.; Nygaard, H.B.; Gilbert, J.W.; Strittmatter, S.M., Cellular Prion Protein Mediates Impairment of Synaptic Plasticity by Amyloid-b Oligomers. *Nature* **2009**, *457*, 1128-1132.

(22) Chen, S.; Yadav, S.P.; Surewicz, W.K., Interaction between Human Prion Protein and Amyloid-β(Aβ) Oligomers. *J. Biol. Chem.* **2010**, *285*, 26377-26383.

(23) Fluharty, B.R.; Biasini, E.; Stravalaci, M.; Sclip, A.; Diomede, L.; Balducci, C.;

Vitola, P.L.; Messa, M.; Colombo, L.; Forloni, G.; Borsello, T.; Gobbi, M.; Harris, D.A., An N-Terminal Fragment of the Prion Protein Binds to Amyloid-β Oligomers and Inhibits Their Neurotoxicity in vivo. *J. Biol. Chem.* **2013**, *288*, 7857–7866.

(24) Guillot-Sestier, M.V.; Sunyach, C.; Ferreira, S.T.; Marzolo, M.P.; Bauer, C.; Thevenet, A.; Checler, F., α-Secretase-Derived Fragment of Cellular Prion, N1, Protects against Monomeric and Oligomeric Amyloid β (Aβ)-Associated Cell Death. *J. Biol. Chem.* **2012**, *287*, 5021-5032.

(25) Laurén, J., Cellular Prion Protein as A Therapeutic Target in Alzheimer's Disease. *J. Alzheimer's Dis.* **2014**, *38*, 227-244.

(26) Li, D.; Song, S.P.; Fan, C.H., Target-Responsive Structural Switching for Nucleic Acid-Based Sensors. *Acc. Chem. Res.* **2010**, *43*, 631-641.

(27) Wang, J., Electrochemical Glucose Biosensors. *Chem. Rev.* **2008**, *108*, 814-825.

(28) Chen, A.C.; Chatterjee, S., Nanomaterials Based Electrochemical Sensors for Biomedical Applications. *Chem. Soc. Rev.* **2013**, *42*, 5425-5438.

(29) Song, W.; Li, H.; Liang, H.; Qiang, W.; Xu, D., Disposable Electrochemical Aptasensor Array by Using in Situ DNA Hybridization Inducing Silver Nanoparticles Aggregate for Signal Amplification. *Anal. Chem.* **2014**, *86*, 2775-2783.

(30) Wang, H.; Li, G.; Zhang, Y.; Zhu, M.; Ma, H.; Du, B.; Wei, Q.; Wan, Y., Nanobody-Based Electrochemical Immunoassay for Ultrasensitive Determination of Apolipoprotein-A1 Using Silver Nanoparticles Loaded Nanohydroxyapatite as Label. *Anal. Chem.* **2015**, *87*, 11209-11214.

(31) Xia, F.; White, R.; Zuo, X.; Patterson, A.; Xiao, Y.; Kang, D.; Gong, X.; Plaxco, K.; Heeger, A., An Electrochemical Supersandwich Assay for Sensitive and Selective DNA Detection in Complex Matrices. *J. Am. Chem. Soc.* **2010**, *132*, 14346-14348.

(32) Zhang, B.; Liu, B.; Zhou, J.; Tang, J.; Tang, D., Additional Molecular Biological Amplification Strategy for Enhanced Sensitivity of Monitoring Low-Abundance Protein with Dual Nanotags. *ACS Appl. Mater. Interfaces* **2013**, *5*, 4479-4485.

(33) Li, X.; Scida, K.; Crooks, R.M., Detection of Hepatitis B Virus DNA with a Paper Electrochemical Sensor. *Anal. Chem.* **2015**, *87*, 9009-9015.

(34) Lin, D.; Wu, J.; Wang, M.; Yan, F.; Ju, H., Triple Signal Amplification of Graphene Film, Polybead Carried Gold Nanoparticles as Tracing Tag and Silver

Deposition for Ultrasensitive Electrochemical Immunosensing. *Anal. Chem.* **2012**, *84*, 3662-3668.

(35) Mei, C.; Lin, D.; Fan, C.; Liu, A.; Wang, S.; Wang, J., Highly Sensitive and Selective Electrochemical Detection of Hg2+ through Surface-Initiated Enzymatic Polymerization. *Biosens. Bioelectron.* **2016**, *80*, 105-110.

(36) Scida, K.; Cunningham, J.C.; Renault, C.; Richards, I.; Crooks, R.M., Simple, Sensitive, and Quantitative Electrochemical Detection Method for Paper Analytical Devices. *Anal. Chem.* **2014**, *86*, 6501-6507.

(37) Singh, P.; Parent, K.L.; Buttry, D.A., Electrochemical Solid-State Phase Transformations of Silver Nanoparticles. *J. Am. Chem. Soc.* **2012**, *134*, 5610-5617.

(38) He, Y.; Xie, S.; Yang, X.; Yuan, R.; Chai, Y., Electrochemical Peptide Biosensor Based on in Situ Silver Deposition for Detection of Prostate Specific Antigen. *ACS Appl. Mater. Interfaces* **2015**, *7*, 13360-13366.

(39) Miao, P.; Tang, Y.; Yin, J., MicroRNA Detection Based on Analyte Triggered Nanoparticle Localization on A Tetrahedral DNA Modified Electrode Followed by Hybridization Chain Reaction Dual Amplification. *Chem. Commun.* **2015**, *51*, 15629-15632.

(40) Miao, P.; Wang, B.; Meng, F.; Yin, J.; Tang, Y., Ultrasensitive Detection of MicroRNA through Rolling Circle Amplification on a DNA Tetrahedron Decorated Electrode. *Bioconjugate Chem.* **2015**, *26*, 602-607.

(41) Wei, T.; Dong, T.; Wang, Z.; Bao, J.; Tu, W.; Dai, Z., Aggregation of Individual Sensing Units for Signal Accumulation: Conversion of Liquid-Phase Colorimetric Assay into Enhanced Surface-Tethered Electrochemical Analysis. *J. Am. Chem. Soc.* **2015**, *137*, 8880-8883.

(42) Hu, Q.-D.; Tang, G.-P.; Chu, P.K., Cyclodextrin-Based Host−Guest Supramolecular Nanoparticles for Delivery: From Design to Applications. *Acc. Chem. Res.* **2014**, *47*, 2017-2025.

(43) Yan, H.; He, L.; Zhao, W.; Li, J.; Xiao, Y.; Yang, R.; Tan, W., Poly β-Cyclodextrin/TPdye Nanomicelle-based Two-Photon Nanoprobe for Caspase‑3 Activation Imaging in Live Cells and Tissues. *Anal. Chem.* **2014**, *86*, 11440-11450.

(44) Gao, J.; Guo, Z.; Su, F.; Gao, L.; Pang, X.; Cao, W.; Du, B.; Wei, Q.,

Ultrasensitive Electrochemical Immunoassay for CEA through Host–Guest Interaction of β-Cyclodextrin Functionalized Graphene and Cu@Ag Core–Shell Nanoparticles with Adamantine-Modified Antibody. *Biosens. Bioelectron.* **2015**, *63*, 465-471.

(45) Wang, L.; Lei, J.; Ma, R.; Ju, H., Host−Guest Interaction of Adamantine with a β-Cyclodextrin-Functionalized AuPd Bimetallic Nanoprobe for Ultrasensitive Electrochemical Immunoassay of Small Molecules. *Anal. Chem.* **2013**, *85*, 6505-6510.

(46) Kim, J.A.; Kim, M.; Kang, S.M.; Lim, K.T.; Kim, T.S.; Kang, J.Y., Magnetic Bead Droplet Immunoassay of Oligomer Amyloid Beta for the Diagnosis of Alzheimer's Disease Using Micro-Pillars to Enhance the Stability of the Oil-Water Interface. *Biosens. Bioelectron.* **2015**, *67* 724-732.

(47) Wang, X.; Wu, L.; Ren, J.; Miyoshi, D.; Sugimoto, N.; Qu, X., Label-free Colorimetric and Quantitative Detection of Cancer Marker Protein Using Noncrosslinking Aggregation of Au/Ag Nanoparticles Induced by Target-Specific Peptide Probe. *Biosens. Bioelectron.* **2011**, *26*, 4804-4809.

(48) Wei, H.; Chen, C.; Han, B.; Wang, E., Enzyme Colorimetric Assay Using Unmodified Silver Nanoparticles. *Anal. Chem.* **2008**, *80*, 7051-7055.

(49) Pradhan, N.; Jana, D.; Ghorai, B.K.; Jana, N.R., Detection and Monitoring of Amyloid Fibrillation Using a Fluorescence “Switch-On” Probe. *ACS Appl. Mater. Interfaces* **2015**, *7*, 25813-25820.

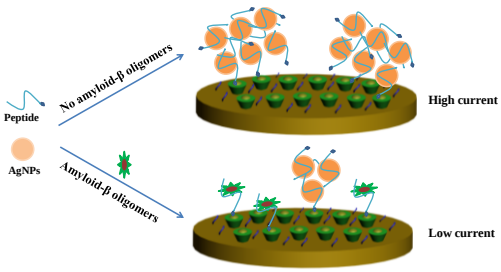
Peptide
AgNPs
No amyloid-β oligomers
Amyloid-β oligomers
High current
Low current